Physica A 518 (2019) 30–37

Contents lists available at ScienceDirect

Physica A

journal homepage: www.elsevier.com/locate/physa

Controlled drug release from a spheroidal matrix

Laurent Simon [a,*], Juan Ospina [b]

[a] Otto H. York Department of Chemical and Materials Engineering, New Jersey Institute of Technology, Newark NJ 07102, USA
[b] Logic and Computation Group, Physics Engineering Program, School of Sciences and Humanities, EAFIT University, Medellin, Colombia

HIGHLIGHTS

- The effective time constant was calculated for a prolate spheroidal device.
- An analytical solution was derived for the fraction of drug released.
- The effective time constant was expressed as a function of the aspect ratio.

ARTICLE INFO

Article history:
Received 17 June 2018
Received in revised form 8 September 2018
Available online 29 November 2018

Keywords:
Effective time constant
Controlled release
Spheroidal matrix
Laplace transform
Legendre polynomials

ABSTRACT

Drug transport through a spheroidal matrix was studied using Fick's second law *of diffusion in spherical coordinates.* The *prolate spheroid-shaped* geometry was described by a small angular deformation applied at the surface of the body. An infinite series of Legendre polynomials of order two was first used to develop an expression for the solute concentration in the Laplace domain. This method resulted in closed-form expressions for the effective time constant and the cumulative percentage of drug released in terms of critical model parameters. The procedure predicted published solutions very well. More moisture was observed at the center of the body when compared to the focal point. As the aspect ratio increased, the effective time constant decreased. At 0.38 unit time, 98.6% of the loaded drug was released from the device.

1. Introduction

The modeling of controlled drug-release is routinely performed for flat plates, spheres and cylinders. For complex geometries, theoretical analyses are rare due, in part, to the difficulty in deriving closed-formed solutions. In addition, traditional mathematical methods are developed for Cartesian, cylindrical and spherical coordinate systems [1]. This trend results in the lack of performance metrics that could promote the design of devices in the form of spheroids. For example, expressions are available for estimating the steady-state transdermal flux or the lag time for drug release into the bloodstream via the skin when a patch is applied [2,3]. However, the calculations would be more elaborate for ellipsoids, such as the ones described by De Lima and Nebra [4].

This contribution focuses on the problem of diffusive transport through a prolate spheroid, a surface obtained by revolving an ellipse about its major axis. The approach represents a more realistic situation, not observed in the idealization of matrices as spheres, and would allow researchers to create more accurate simulations. A main impetus, for the proposed work, is the breadth of research that targets therapeutic drug delivery across protective barriers that are closer to a spheroid, in shape, than a perfect sphere. Potential areas of applications are (i) the controlled delivery of exogenous molecules applied topically

* Corresponding author.
E-mail address: laurent.simon@njit.edu (L. Simon).

https://doi.org/10.1016/j.physa.2018.11.048
0378-4371/

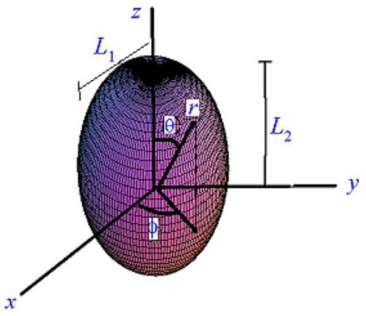

Fig. 1. Schematic representation of the prolate spheroidal matrix.

to the eye, (ii) the fabrication of implantable releasing devices and (iii) the design of drugs administered to kill cancer cells in a solid tumor. In the case of ocular drug delivery, the corneal layers are major barriers to transport [5] and, according to several reports, the cornea is best represented by a prolate spheroid [6–8]. Ellipsoidal-shaped implants are placed under the lower cul-de-sac of the eye to release a certain amount of pilocarpine for seven days [9]. The mechanism of how an anticancer drug is transported to the tumor spheroids and its subsequent diffusion through the capillaries is of great importance in chemotherapy [10,11].

A method is provided to explore the dynamics of a compound diffusing through a biological or synthetic membrane in the shape of a prolate spheroid. The rate at which the drug molecules exits the capsule, i.e., the system converges to equilibrium, is calculated.

2. Theory

2.1. Mathematical modeling

A pharmaceutical ingredient of concentration c_0 is uniformly distributed within a prolate spheroidal matrix (Fig. 1). The surface of the device is maintained at zero. This assumption is referred to as the perfect sink condition imposed for a highly dilute reservoir. The transport of drug in the polymer is mainly governed by Fick's second law of diffusion in spherical coordinates:

$$\frac{\partial c\left(r,\theta,t\right)}{\partial t}=\frac{K}{r^2}\left[\frac{\partial}{\partial r}\left(r^2\frac{\partial c}{\partial r}\right)+\frac{1}{\sin\left(\theta\right)}\frac{\partial}{\partial\theta}\left(\sin\left(\theta\right)\frac{\partial c}{\partial r}\right)\right] \tag{1}$$

where t is the time, c is the drug concentration in the matrix, r is the radial distance, θ is the azimuthal angle and K is the diffusion coefficient. The prolate spheroid-shaped geometry is captured by imposing the following condition at the surface [12]:

$$r=R\left(1+\varepsilon P_2\left(\cos\left(\theta\right)\right)\right) \tag{2}$$

where $P_2\left(x\right)$ is the Legendre polynomial of order two at x defined by $P_2\left(x\right)=\frac{3x^2}{2}-\frac{1}{2}$; R is the radius of the perfect sphere from which the spheroid is generated after applying a small angular deformation of size $\varepsilon RP_2\left(\cos\left(\theta\right)\right)$; ε is a constant that specifies the extent of the deviation.

Based on Fig. 1, the following two equations are derived:

$$\frac{L_2}{L_1}=\frac{1}{\sqrt{1-3\varepsilon}} \tag{3}$$

and

$$\Delta=R\sqrt{\frac{3\varepsilon\left(\varepsilon-1\right)}{3\varepsilon-1}} \tag{4}$$

with Δ being the distance of the focal point to the center. The initial and boundary conditions are

$$c\left(r,\theta,0\right)=c_0 \tag{5}$$

and

$$c\left(R\left(1+\varepsilon P_2\left(\cos\left(\theta\right)\right)\right),\theta,t\right)=0 \tag{6}$$

respectively.

The volume of the carrier is given by

$$V = 2\pi \int_0^{\pi} \int_0^{R(1+\varepsilon P_2(\cos(\theta)))} r^2 \sin(\theta)\, dr d\theta \tag{7}$$

which simplifies to

$$V = 4\pi R^3 \left(\frac{2}{105}\varepsilon^3 + \frac{1}{5}\varepsilon^2 + \frac{1}{3} \right) \tag{8}$$

The surface of the prolate spheroid is written as

$$A = 2\pi \int_0^{\pi} R^2 \left(1 + \varepsilon P_2(\cos(\theta))\right)^2 \sin(\theta)\, d\theta \tag{9}$$

or

$$A = 4\pi R^2 \left(\frac{1}{5}\varepsilon^2 + 1 \right) \tag{10}$$

It is of interest to calculate the cumulative amount of drug released at each time point. This measure is obtained by taking the difference between the initial mass and the amount remaining in the matrix:

$$M(t) = 4\pi R^3 c_0 \left(\frac{2}{105}\varepsilon^3 + \frac{1}{5}\varepsilon^2 + \frac{1}{3} \right) - 2\pi \int_0^{\pi} \int_0^{R(1+\varepsilon P_2(\cos(\theta)))} c(r, \theta, t)\, r^2 \sin(\theta)\, dr d\theta \tag{11}$$

2.2. Dynamic properties

2.2.1. Transient behavior

In the Laplace domain, Eq. (1) takes the form

$$sC(r,\theta) - c_0 = K \frac{\partial^2}{\partial r^2} C(r,\theta) + 2\frac{K\frac{\partial}{\partial r}C(r,\theta)}{r} + \frac{K\frac{\partial^2}{\partial \theta^2}C(r,\theta)}{r^2} + \frac{K\cos(\theta)\frac{\partial}{\partial \theta}C(r,\theta)}{\sin(\theta)\, r^2} \tag{12}$$

where

$$C(r,\theta) = \int_0^{\infty} c(r,\theta,t)\, e^{-st} dt \tag{13}$$

using the initial condition (5).

The general solution of Eq. (12) is given by

$$C(r,\theta) = \frac{c_0}{s} + \sum_{L=0}^{\infty} \frac{C_L P_L(\cos(\theta)) J_{L+\frac{1}{2}}\left(\sqrt{-\frac{s}{K}} r\right)}{\sqrt{r}} \tag{14}$$

where $P_n(x)$ is the Legendre polynomial of order n at x, $J_n(x)$ gives the Bessel function of the first kind and C_L is a constant to be determined.

The Laplace transform of the boundary condition (6) yields

$$\frac{c_0}{s} + \sum_{L=0}^{\infty} \frac{C_L P_L(\cos(\theta)) J_{L+\frac{1}{2}}\left(\sqrt{-\frac{s}{K}} R\left(1 + \varepsilon P_2(\cos(\theta))\right)\right)}{\sqrt{R\left(1 + \varepsilon P_2(\cos(\theta))\right)}} = 0 \tag{15}$$

Conserving only the first two even terms in the summation in Eq. (15), we obtain

$$\frac{c_0}{s} + \frac{C_0 J_{\frac{1}{2}}\left(\sqrt{-\frac{s}{K}} R\left(1 + \varepsilon P_2(\cos(\theta))\right)\right)}{\sqrt{R\left(1 + \varepsilon P_2(\cos(\theta))\right)}} + \frac{C_2 P_2(\cos(\theta)) J_{\frac{5}{2}}\left(\sqrt{-\frac{s}{K}} R\left(1 + \varepsilon P_2(\cos(\theta))\right)\right)}{\sqrt{R\left(1 + \varepsilon P_2(\cos(\theta))\right)}} = 0 \tag{16}$$

After expressing the Bessel functions in terms of trigonometric function, performing a series expansion of Eq. (16) around $\varepsilon = 0$ up to order 2, and collecting the terms with Legendre polynomials, we have

$$A_0 + A_2 P_2(\cos(\theta)) = 0 \tag{17}$$

with

$$A_0 = \frac{c_0}{s} + \frac{C_0\sqrt{2}\sin\left(\sqrt{-\frac{s}{K}} R\right)}{\sqrt{\pi R}\sqrt{\sqrt{-\frac{s}{K}} R}} \tag{18}$$

and

$$A_2 = -\frac{C_2\sqrt{2}}{\sqrt{\pi}sR^{5/2}}\left(\sin\left(\sqrt{-\frac{s}{K}}R\right)\sqrt{-\frac{s}{K}}sR^2+3\sin\left(\sqrt{-\frac{s}{K}}R\right)\sqrt{-\frac{s}{K}}K+3\cos\left(\sqrt{-\frac{s}{K}}R\right)sR\right)\frac{1}{\sqrt{\sqrt{-\frac{s}{K}}R}}\frac{1}{\sqrt{-\frac{s}{K}}}+ \varepsilon\left(-\frac{1}{2}\frac{C_0\sqrt{2}}{\sqrt{\pi}\sqrt{R}}\sin\left(\sqrt{-\frac{s}{K}}R\right)\frac{1}{\sqrt{\sqrt{-\frac{s}{K}}R}}\right)+ \frac{\varepsilon}{\sqrt{R}}\left(\frac{C_0\sqrt{2}R}{\sqrt{\pi}}\cos\left(\sqrt{-\frac{s}{K}}R\right)\sqrt{-\frac{s}{K}}\frac{1}{\sqrt{\sqrt{-\frac{s}{K}}R}}-1/2\frac{C_0\sqrt{2}}{\sqrt{\pi}}\sin\left(\sqrt{-\frac{s}{K}}R\right)\frac{1}{\sqrt{\sqrt{-\frac{s}{K}}R}}\right) \tag{19}$$

In this representation, it is assumed that the deviation of the body from a perfect spherical shape is small: $R \gg \varepsilon$ and $P_2(\cos(\theta))^2 \approx 0$. The coefficients C_0 and C_2 are obtained by first setting $A_0 = A_2 = 0$ (see Eq. (17)) and solving Eqs. (18) and (19):

$$C_0 = -\frac{1}{2}\frac{c_0\sqrt{2\pi R}\sqrt{\sqrt{-\frac{s}{K}}R}}{\sin\left(\sqrt{-\frac{s}{K}}R\right)s} \tag{20}$$

and

$$C_2 = \frac{1}{2}\frac{c_0\sqrt{2\pi}R^{5/2}\epsilon\sqrt{\sqrt{-\frac{s}{K}}R}\left(\sin\left(\sqrt{-\frac{s}{K}}R\right)\sqrt{-\frac{s}{K}}K+\cos\left(\sqrt{-\frac{s}{K}}R\right)sR\right)}{K\sin\left(\sqrt{-\frac{s}{K}}R\right)\left(\sin\left(\sqrt{-\frac{s}{K}}R\right)\sqrt{-\frac{s}{K}}sR^2+3\sin\left(\sqrt{-\frac{s}{K}}R\right)\sqrt{-\frac{s}{K}}K+3\cos\left(\sqrt{-\frac{s}{K}}R\right)sR\right)} \tag{21}$$

Therefore, the concentration is

$$C(r,\theta) = \frac{c_0}{s}+\frac{C_0J_{\frac{1}{2}}\left(\sqrt{-\frac{s}{K}}r\right)}{\sqrt{r}}+\frac{C_2P_2(\cos(\theta))J_{\frac{5}{2}}\left(\sqrt{-\frac{s}{K}}r\right)}{\sqrt{r}} \tag{22}$$

with C_0 and C_2 defined by Eqs. (20) and (21), respectively. Eq. (22) is further simplified to

$$C(r,\theta) = \frac{c_0}{s}-\frac{c_0R\sinh\left(\frac{\sqrt{s}r}{\sqrt{K}}\right)}{sr\sinh\left(\frac{\sqrt{s}R}{\sqrt{K}}\right)}- \frac{\left(c_0R^3\epsilon P_2(\cos(\theta))\left(\sinh\left(\frac{\sqrt{s}R}{\sqrt{K}}\right)\sqrt{s}\sqrt{K}-\cosh\left(\frac{\sqrt{s}R}{\sqrt{K}}\right)sR\right)\times\left(\sinh\left(\frac{\sqrt{s}r}{\sqrt{K}}\right)s^{3/2}r^2+3\sinh\left(\frac{\sqrt{s}r}{\sqrt{K}}\right)\sqrt{s}K-3\cosh\left(\frac{\sqrt{s}r}{\sqrt{K}}\right)sr\sqrt{K}\right)\right)}{s^{3/2}\sqrt{K}r^3\sinh\left(\frac{\sqrt{s}R}{\sqrt{K}}\right)\left(\sinh\left(\frac{\sqrt{s}R}{\sqrt{K}}\right)s^{3/2}R^2+3\sinh\left(\frac{\sqrt{s}R}{\sqrt{K}}\right)\sqrt{s}K-3\cosh\left(\frac{\sqrt{s}R}{\sqrt{K}}\right)sR\sqrt{K}\right)} \tag{23}$$

The solution above is of the form $C(r,\theta) = C_{PS}(r,\theta)+\varepsilon\gamma P_2(\cos(\theta))$ where γ is a measure of how much the body deviates from a perfect sphere and $C_{PS}(r,\theta)$ is the solution for the perfect sphere.

The Laplace transform of $M(t)$ is

$$\overline{M}(s) = 4\pi R^3c_0\left(\frac{2}{105}\varepsilon^3+\frac{1}{5}\varepsilon^2+\frac{1}{3}\right)\frac{1}{s}-2\pi\int_0^{\pi}\int_0^{R(1+\varepsilon P_2(\cos(\theta)))}C(r,\theta)\,r^2\sin(\theta)\,drd\theta \tag{24}$$

The infinite value is

$$M(\infty) = \lim_{t\to\infty}M(t) = \lim_{s\to 0}s\overline{M}(s) = 4\pi R^3c_0\left(\frac{2}{105}\varepsilon^3+\frac{1}{5}\varepsilon^2+\frac{1}{3}\right) \tag{25}$$

and the fractional amount of drug released, in the Laplace domain, is

$$\frac{\overline{M}(s)}{M(\infty)} = \frac{1}{s}-\frac{105}{2}\left(\frac{1}{R^3\left(35+2\varepsilon^3+21\varepsilon^2\right)c_0}\int_0^{\pi}\int_0^{R(1+\varepsilon P_2(\cos(\theta)))}C(r,\theta)\,r^2\sin(\theta)\,drd\theta\right) \tag{26}$$

A numerical technique [13] is applied to invert Eqs. (23) and (26) and determine $c(r,\theta,t)$ and $M(t)/M(\infty)$, respectively. The fixed Talbot (FT) algorithm is based on the deformation of the standard contour in the Bromwich inversion integral [14]:

$$f(t) = \frac{1}{2\pi i}\int_B e^{ts}\hat{f}(s)\,ds \tag{27}$$

where $\hat{f}(s)$ is the Laplace transform of $f(t)$. The contour B is a vertical line such that $s = r + iy$ where $-\infty < y < +\infty$ and r has a fixed value selected so that all the singularities for the inverse Laplace transform are to the left of B. It can be shown that [13]

$$f(t, M) = \frac{r}{M}\left\{\frac{1}{2}\hat{f}(r)\, e^{rt} + \sum_{k=1}^{M-1} \mathrm{Re}\left[e^{ts(\theta_k)}\hat{f}(s(\theta_k))\,(1 + i\sigma(\theta_k))\right]\right\} \tag{28}$$

with

$$\sigma(\theta) = \theta + (\theta\cot\theta - 1)\cot\theta \tag{29}$$

and

$$\theta_k = \frac{k\pi}{M}; \quad r = \frac{2M}{5t} \tag{30}$$

2.2.2. Derivation of the time constant

The time constant, an important performance parameter, is applied to evaluate the characteristic time of a system [15,16]. It can be configured in the construction and validation of biosensors [17]. A first-moment relaxation time constant is defined by [18–20]

$$t_{eff} = \int_0^\infty t\,\Omega(t)\, dt \tag{31}$$

where $\Omega(t)$ represents the probability density function:

$$\Omega(t) = \frac{(\Psi_e - \Psi(t))}{\int_0^\infty (\Psi_e - \Psi(t))\, dt} \tag{32}$$

In Eq. (32), Ψ_e is the steady-state value of Ψ. Another form of Eq. (31) is

$$t_{eff} = \lim_{s\to 0}\left(\frac{\Psi_e}{s^2} + \frac{d\overline{\Psi}(s)}{ds}\right)\left[\lim_{s\to 0}\left(\frac{\Psi_e}{s} - \overline{\Psi}(s)\right)\right]^{-1} \tag{33}$$

where $\overline{\Psi}$ is the Laplace transform of $\Psi(t)$. The final expression for t_{eff} from Eq. (31) or (33) depends on the model parameters. This information allows researchers to investigate the effects of key system properties on t_{eff}. It can be shown that

$$t_{eff} = -\frac{R^2\left(85500\varepsilon^8 + 610470\varepsilon^7 + 1835337\varepsilon^6 + 1790100\varepsilon^5 + 722007\varepsilon^4 - 486200\varepsilon^3 - 1429428\varepsilon^2 - 1361360\right)}{7140K\left(318\varepsilon^6 + 1404\varepsilon^5 + 3861\varepsilon^4 + 2002\varepsilon^3 + 3003\varepsilon^2 + 2002\right)} \tag{34}$$

after using $\Psi_e = 1$ and $\overline{\Psi}(s) = \overline{M}(s)/M(\infty)$. Note that, when $\varepsilon = 0$, Eq. (34) reduces to the time constant of a spherical matrix:

$$t_{sp,eff} = \frac{2R^2}{21K} \tag{35}$$

Moreover, Eq. (34) takes the form

$$t_{eff} = \frac{2R^2}{21K} - \frac{3R^2\varepsilon^2}{70K} \tag{36}$$

for a very small ε, which shows that t_{eff} for the prolate spheroid is less than that of the sphere. Eq. (36) is a truncated series expansion of Eq. (34), with respect to the variable ε, about 0 and up to order 3. It is relevant, for design purposes, to express t_{eff} in terms of the aspect ratio, defined as $\delta = \sqrt{1/(1-3\varepsilon)}$. Eq. (34) becomes:

$$t_{eff} = \frac{R^2\left(\begin{array}{l}1107425818\delta^{16} - 205593332\delta^{14} + 30405145\delta^{12} + 110928742\delta^{10} - \\ 68666768\delta^8 + 21187612\delta^6 - 3525767\delta^4 + 279490\delta^2 - 9500\end{array}\right)}{21420\delta^4 K\left(598678\delta^{12} - 270204\delta^{10} + 220263\delta^8 - 80510\delta^6 + 20193\delta^4 - 2040\delta^2 + 106\right)} \tag{37}$$

When $\delta = 1$, Eq. (37) reduces to Eq. (35). In the limit, when $\delta \to \infty$, the time constant for a needle is obtained:

$$t_{eff} = \frac{0.086R^2}{K} \tag{38}$$

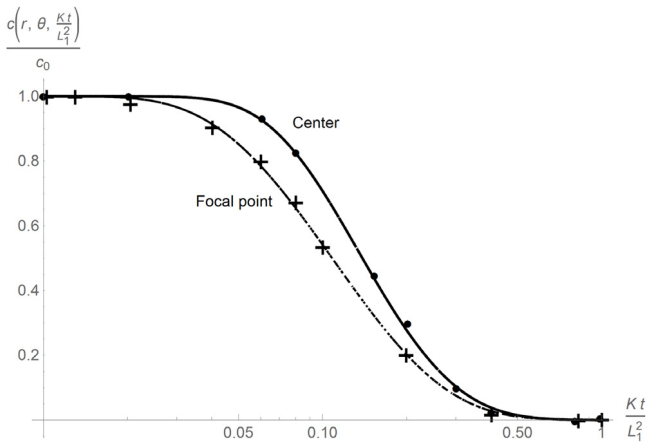

Fig. 2. The normalized moisture contents at the center (___) and at the focal point (- - - - -) of a spheroid with a ratio $L_2/L_1 = 1.1$. The results of Oliveira and Lima [21] are noted by • (center point) and + (focal point).

3. Results and discussions

3.1. Validation of the solution method

The work of Oliveira and Lima is used here to test the accuracy of the solution method [21]. In their contribution, the authors described the drying kinetics and distribution in the moisture content of a prolate spheroid with a ratio L_2/L_1 equal to 1.1 and $R = 1.0$. The initial and boundary conditions of the problem described in [21] are those of the controlled-release system outlined in Section 2.1, i.e., constant properties and boundary conditions at the surface. This problem can also be applied for heat conduction from spheroids [22]. Their results matched the analytical normalized concentration in the center $c\,(0, \theta, \tau)\,/c_0$ and focal point $c\,(\Delta, 0, \tau)\,/c_0$ of the spheroid studied in [21]. A dimensionless time variable, defined as Kt/L_1^2, was used. The focal point corresponds to $r = \Delta$ (see Eq. (4)). The procedure presented in Section 2.2.1 predicted the published solutions very well (Fig. 2). Ample moisture is noted at the center of the body when compared to the focal point. This is because the latter location is closer to the surface where the concentration is maintained at zero. The form of Eq. (28) makes it possible to employ the method with regression algorithms to extract the diffusion coefficient after fitting drying experimental data to the expression for $M\,(t)\,/M\,(\infty)$.

3.2. Cumulative fraction of drug released and time constant

The cumulative fraction of drug released is shown in Fig. 3; the dimensionless effective time constant is 0.095. The value of $M\,(t)\,/M\,(\infty)$ at $4 \times t_{eff}$ is 98.6%, which means that it takes approximately 0.38 unit time for the device to release 98.6% of the loaded drug. This behavior is characteristic of a first-order process where 98% of the steady-state is achieved in $4 \times t_{eff}$ after a unit step change in the input [19,23]. The result is the same if Eq. (36) is applied to estimate t_{eff} based on $L_2/L_1 = 1.1$ or $\varepsilon = 0.058$. Immediate applications of the findings are ocular drug delivery, fabrication of ellipsoidal-shaped implants and transport of an anticancer drug to tumor spheroids.

Fig. 4 depicts how t_{eff} depends on the size of the deviation. As ε is increased, t_{eff} decreases. This curve can be used by researchers as a way to predict t_{eff} or to assess the error in this performance metric if a device is approximated by a perfect sphere instead of a prolate spheroid. Fig. 5 shows the curve for t_{eff} in terms of δ.

4. Conclusions

A mathematical model was developed to analyze the diffusive transport of an active pharmaceutical ingredient through a prolate spheroid. The interest in this specific problem was motivated by the need to represent, accurately, the transport through prolate spheroid structures, such as the cornea. The drug was uniformly distributed within the matrix while the concentration at the surface of the device was kept at zero. Transport in the polymer was best represented by Fick's second law of diffusion in spherical coordinates. An infinite series of Legendre polynomials of order two was applied and led to an analytical expression for the solute concentration in the Laplace domain. The solution contained two terms. One of which was the solution for the perfect sphere and the other, a function of the azimuthal angle. The methodology yielded a single effective time constant and the cumulative fraction of drug released for small deviations of the spheroid from a perfect sphere. Estimated concentration at the center and the focal point agreed very well with published data and showed that more moisture is located at the center of the spheroid. An increase in the aspect ratio led to a reduction in the effective time constant. At 0.38 unit time or four time constants, 98.6% of the loaded drug was released from the device, a behavior that is characteristic of a first-order system.

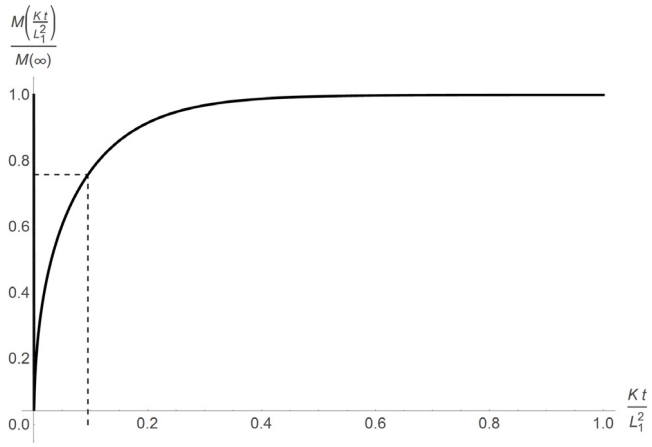

Fig. 3. The cumulative fraction of drug released (___) and the dimensionless effective time constant (- - - - -).

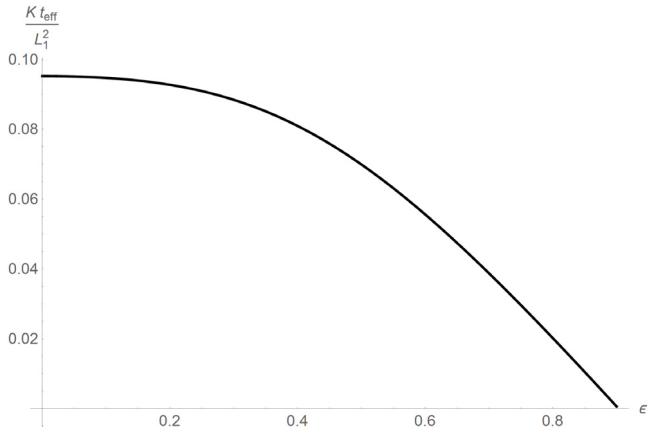

Fig. 4. The effective time constant as a function of ε (see Eq. (30)).

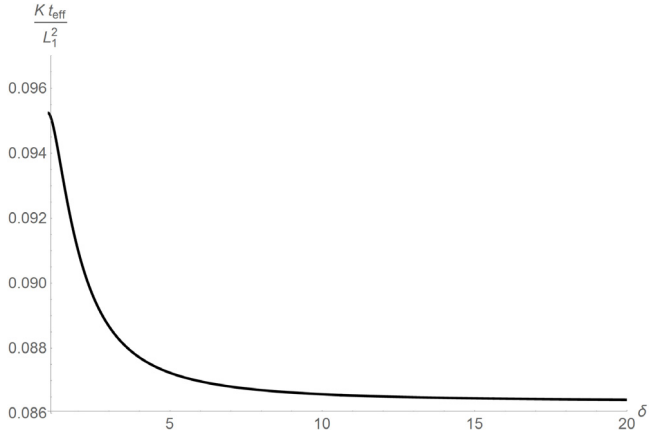

Fig. 5. The effective time constant as a function of the aspect ratio δ (see Eq. (33)).

References

[1] J. Crank, The Mathematics of Diffusion, second ed., Clarendon Press, Oxford, Eng, 1975.
[2] E.H. Twizell, K. Kubota, Lag time in the dual sorption model for percutaneous absorption with finite skin-receptor boundary clearance, Math. Biosci. 123 (1994) 1–23.

[3] L. Simon, Timely drug delivery from controlled-release devices: dynamic analysis and novel design concepts, Math. Biosci. 217 (2009) 151–158.
[4] A.G.B. De Lima, S.A. Nebra, Theoretical analysis of the diffusion process inside prolate spheroidal solids, Drying Technol. 18 (2000) 21–48.
[5] R. Gaudana, H.K. Ananthula, A. Parenky, A.K. Mitra, Ocular drug delivery, AAPS J. 12 (2010) 348–360.
[6] S.A. Read, M.J. Collins, L.G. Carney, R.J. Franklin, The topography of the central and peripheral cornea, Invest. Ophthalmol. Vis. Sci. 47 (2006) 1404–1415.
[7] L.G. Carney, J.C. Mainstone, B.A. Henderson, Corneal topography and myopia. A cross-sectional study, Invest. Ophthalmol. Vis. Sci. 38 (1997) 311–320.
[8] R.J. Braun, R. Usha, G.B. McFadden, T.A. Driscoll, L.P. Cook, P.E. King-Smith, Thin film dynamics on a prolate spheroid with application to the cornea, J. Eng. Math. 73 (2012) 121–138.
[9] F. Puoci, Advanced Polymers in Medicine, Springer International Publishing, 2014.
[10] H. Namazi, V.V. Kulish, A. Wong, S. Nazeri, Mathematical based calculation of drug penetration depth in solid tumors, Biomed. Res. Int. 2016 (2016) 8.
[11] M.E. Ackerman, D. Pawlowski, K.D. Wittrup, Effect of antigen turnover rate and expression level on antibody penetration into tumor spheroids, Mol. Cancer Ther. 7 (2008) 2233–2240.
[12] J. Jeans, The Mathematical Theory of Electricity and Magnetism, fifth ed., The University Press, Cambridge Eng, 1925.
[13] J. Abate, P.P. Valkó, Multi-precision Laplace transform inversion, Internat. J. Numer. Methods Engrg. 60 (2004) 979–993.
[14] A. Talbot, The accurate numerical inversion of laplace transforms, IMA J. Appl. Math. 23 (1979) 97–120.
[15] L. Simon, J. Ospina, Closed-Form Solutions for Drug Transport through Controlled-Release Devices in Two and Three Dimensions, John Wiley & Sons Inc., Hoboken, New Jersey, 2015.
[16] J.A. Ferreira, P. de Oliveira, P. da Silva, L. Simon, Flux tracking in drug delivery, Appl. Math. Model. 35 (2011) 4684–4696.
[17] D.R. Thevenot, K. Toth, R.A. Durst, G.S. Wilson, Electrochemical biosensors: recommended definitions and classification, Biosens. Bioelectron. 16 (2001) 121–131.
[18] R. Collins, The choice of an effective time constant for diffusive processes in finite systems (Thermal conduction and sputtering examples), J. Phys. D: Appl. Phys. 13 (1980) 1935.
[19] L. Simon, Control of Biological and Drug-Delivery Systems for Chemical, Biomedical, and Pharmaceutical Engineering, Wiley, Hoboken, NJ, 2013.
[20] L. Simon, J. Ospina, On the effusion time of drugs from the open pore of a spherical vesicle, Physica A 451 (2016) 366–372.
[21] V.A.B. Oliveira, A.G.B. Lima, Mass diffusion inside prolate spherical solids: an analytical solution, Rev. Brasil. Produtos Agroindustriais, Campina Grande 4 (2002) 41–50.
[22] A. Haji-Sheikh, E.M. Sparrow, Transient heat conduction in a prolate spheroidal solid, J. Heat Transfer 88 (1966) 331–333.
[23] C.A. Smith, A.B. Corripio, Principles and Practice of Automatic Process Control, third ed., Wiley, Hoboken, NJ, 2006.